THE JOURNAL OF PHYSICAL CHEMISTRY A

ARTICLE

pubs.acs.org/JPCA

# Prompt $HO_2$ Formation Following the Reaction of OH with Aromatic Compounds under Atmospheric Conditions

Sascha Nehr, Birger Bohn,* and Andreas Wahner

Institut für Energie- und Klimaforschung IEK-8, Troposphäre, Forschungszentrum Jülich GmbH, 52425 Jülich, Germany

**ABSTRACT:** The secondary formation of $HO_2$ radicals following OH + aromatic hydrocarbon reactions in synthetic air under normal pressure and temperature was investigated in the absence of NO after pulsed production of OH radicals. OH and $HO_x$ (=OH + $HO_2$) decay curves were recorded using laser-induced fluorescence after gas-expansion. The prompt $HO_2$ yields ($HO_2$ formed without preceding NO reactions) were determined by comparison to results obtained with CO as a reference compound. This approach was recently introduced and applied to the OH + benzene reaction and was extended here for a number of monocyclic aromatic hydrocarbons. The measured $HO_2$ formation yields are as follows: toluene, 0.42 ± 0.11; ethylbenzene, 0.53 ± 0.10; *o*-xylene, 0.41 ± 0.08; *m*-xylene, 0.27 ± 0.06; *p*-xylene, 0.40 ± 0.09; 1,2,3-trimethylbenzene, 0.31 ± 0.06; 1,2,4-trimethylbenzene, 0.37 ± 0.09; 1,3,5-trimethylbenzene, 0.29 ± 0.08; hexamethylbenzene, 0.32 ± 0.08; phenol, 0.89 ± 0.29; *o*-cresol, 0.87 ± 0.29; 2,5-dimethylphenol, 0.72 ± 0.12; 2,4,6-trimethylphenol, 0.45 ± 0.13. For the alkylbenzenes $HO_2$ is the proposed coproduct of phenols, epoxides, and possibly oxepins formed in secondary reactions with $O_2$. In most product studies the only quantified coproducts were phenols whereas only a few studies reported yields of epoxides. Oxepins have not been observed so far. Together with the yields of phenols from other studies, the $HO_2$ yields determined in this work set an upper limit to the combined yields of epoxides and oxepins that was found to be significant (≤0.3) for all investigated alkylbenzenes except *m*-xylene. For the hydroxybenzenes the currently proposed $HO_2$ coproducts are dihydroxybenzenes. For phenol and *o*-cresol the determined $HO_2$ yields are matching the previously reported dihydroxybenzene yields, indicating that these are the only $HO_2$ forming reaction channels. For 2,5-dimethylphenol and 2,4,6-trimethylphenol no complementary product studies are available.

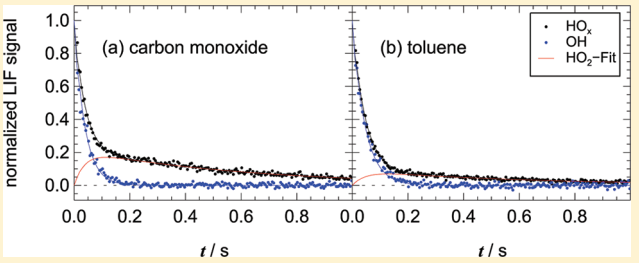


## INTRODUCTION

Aromatic hydrocarbons, such as benzene,[1] alkylbenzenes,[2−5] and hydroxybenzenes,[6,7] comprise a significant fraction of volatile organic compounds observed in urban areas. The emission of aromatics is mostly linked to anthropogenic activities like incomplete combustion of fossil fuels, evaporation from industrial production plants, and residential wood burning.[1,8] During the daytime, the atmospheric degradation of aromatic hydrocarbons is almost exclusively initiated by the reaction with OH radicals[9] and leads to the formation of ozone and secondary organic aerosol.[10,11] Because of their atmospheric lifetimes of up to several days,[12] aromatics impact air quality on a local as well as on a regional scale.[13]

The current understanding of the OH-initiated atmospheric oxidation of alkylbenzenes is depicted in Figure 1 using the example of *o*-xylene. From kinetic experiments and product studies it is known that the OH + alkylbenzene reaction proceeds via (i) reversible OH-addition to the ring, (ii) H-atom abstraction from the C−H bonds (preferentially from substituent alkyl groups), and (iii) dealkylation. The bulk of the reaction (≥90%)[9] proceeds via addition forming an aromatic−OH adduct (in the following briefly referred to as adduct) (Figure 1, A). The H-atom abstraction channel finally yielding benzaldehydes (Figure 1, K, NO reaction step required) and the dealkylation pathway[14,15] (J) are of minor importance. The subsequent reactions of the adduct have been widely studied experimentally.[16−23] Under atmospheric conditions the adduct predominantly reacts with $O_2$ via both reversible addition to give a peroxy radical (adduct-$O_2$, Figure 1, B) and irreversible reaction pathways. Proposed major products are phenols (C),[14,24−27] epoxides (E, F),[27−31] oxepins (I),[32] and a bicyclic peroxy radical (H).[31] The bicyclic peroxy radical can undergo reactions with NO and subsequently with $O_2$, finally yielding ring fragmentation products (e.g., α-dicarbonyls) and $HO_2$.[33] Recent research showed that organic nitrate formation in the bicyclic peroxy radical + NO reaction is a minor channel (<10%).[34] Phenols, epoxides, and oxepins are considered to be the coproducts of prompt $HO_2$; i.e., $HO_2$ formed without the preceding reaction of peroxy radicals with NO. Formation of phenols[14,24−27] and epoxides[27−31] was experimentally confirmed, whereas the oxepin pathway was shown to be inoperative at least for the OH + benzene reaction.[35] There is no experimental evidence for oxepin formation from alkylbenzenes but quantum chemical computations support this pathway.[32] Among the currently proposed prompt $HO_2$ coproducts, only phenols

**Special Issue:** A. R. Ravishankara Festschrift

**Received:** November 14, 2011
**Revised:** December 22, 2011
**Published:** December 23, 2011

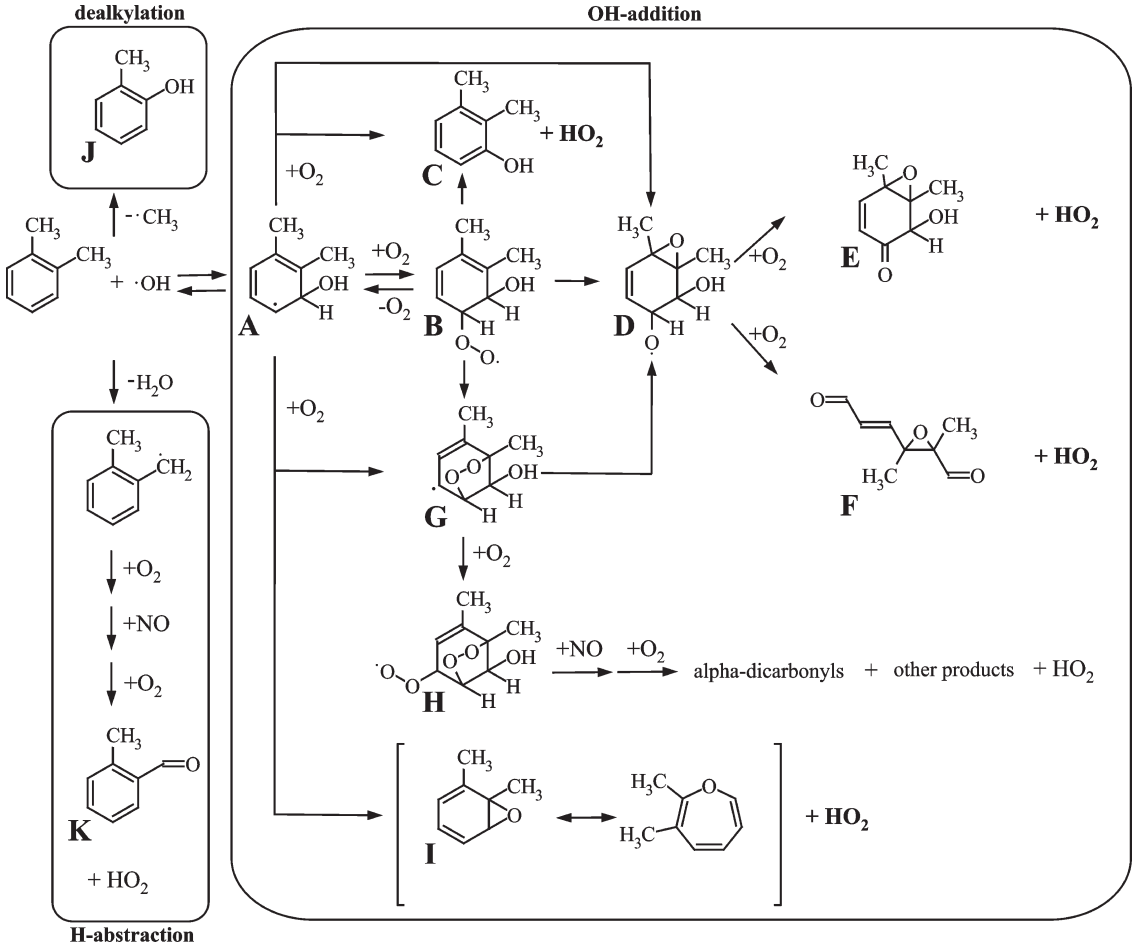


**Figure 1.** Postulated reaction pathways of the OH-initiated oxidation of *o*-xylene.[14,61,66] For convenience, different resonance structures and possible isomers are not shown. $HO_2$ formed without preceding NO reaction steps is indicated in boldface.

were quantified for most of the investigated alkylbenzenes.[14,26] In these cases the measurement of prompt $HO_2$ yields can help set an upper limit to the combined yield of the epoxides and oxepins.

The OH-initiated atmospheric oxidation of hydroxybenzenes is displayed in Figure 2 using the example of *o*-cresol. Reactions proceed via (i) reversible OH-addition to the ring and (ii) H-atom abstraction from the substituent hydroxyl group (H-atom abstraction from the alkyl substituent is negligible).[36] Comparable to the OH + alkylbenzene reaction, the addition pathway is predominant (≥90%) and the H-atom abstraction channel finally yielding nitrophenols (Figure 2, IX, $NO_2$ reaction step required) is of minor importance.[37] Under atmospheric conditions, the subsequent fate of the aromatic−OH adduct is also governed by the reaction with $O_2$. However, the adduct + $O_2$ chemistry is different for hydroxybenzenes and to date no experimental evidence is available for intermediately formed peroxy radicals. Several pathways were proposed for the adduct + $O_2$ reaction depending on the OH-addition site with respect to the existing hydroxyl substituent.[36] Major confirmed products are dihydroxybenzenes (II) most likely stemming from *ortho*-OH-addition followed by direct H-displacement and 1,4-benzoquinones (VI).[36] Formation of 1,4-benzoquinones was assigned to *ipso*-OH-addition, yielding a monocyclic peroxy radical (IV) upon reaction with $O_2$. The peroxy radical can undergo further reactions with NO and subsequently with $O_2$, finally yielding 1,4-benzoquinones. A product study by Olariu et al.[36] suggests that the bulk of the OH + hydroxybenzene reaction (>0.6) proceeds via *ortho*-OH-addition whereas *ipso*-OH-addition is of minor (<0.1) importance. No experimental evidence was reported for *meta*- and/or *para*-OH-addition. Thus, prompt $HO_2$ is proposed to result exclusively from *ortho*-OH-addition. The measurement of prompt $HO_2$ yields can help to experimentally confirm the $HO_2$ forming reaction channels by matching the previously reported[36] formation yield of dihydroxybenzenes.

## EXPERIMENTAL METHODS

The instrument used in this work was originally developed to measure total OH reactivities $k_{OH}$ in ambient air by recording artificial OH decay curves.[38,39] In a recent study performed in our lab,[40] we described modifications of the experimental setup that facilitate the alternating measurement of OH and $HO_x$ (=OH + $HO_2$) decay curves after pulsed formation of OH in the presence of selected reactants. In brief, the apparatus consists of the reaction volume under laminar flow conditions and the OH-detection cell based on the laser-induced fluorescence (LIF) technique. The tube-shaped reaction volume (length = 80 cm, diameter = 4 cm) was operated at atmospheric pressure and 298 K. Highly purified synthetic air entered the reaction volume at a typical flow rate of 20 L $min^{-1}$. Traces of $O_3$ (≈2 × $10^{12}$ $cm^{-3}$, produced by $O_2$ photolysis) and $H_2O$ (≈3 × $10^{17}$ $cm^{-3}$) were added. A fourth harmonic Nd:YAG laser (Big Sky, CFR200),

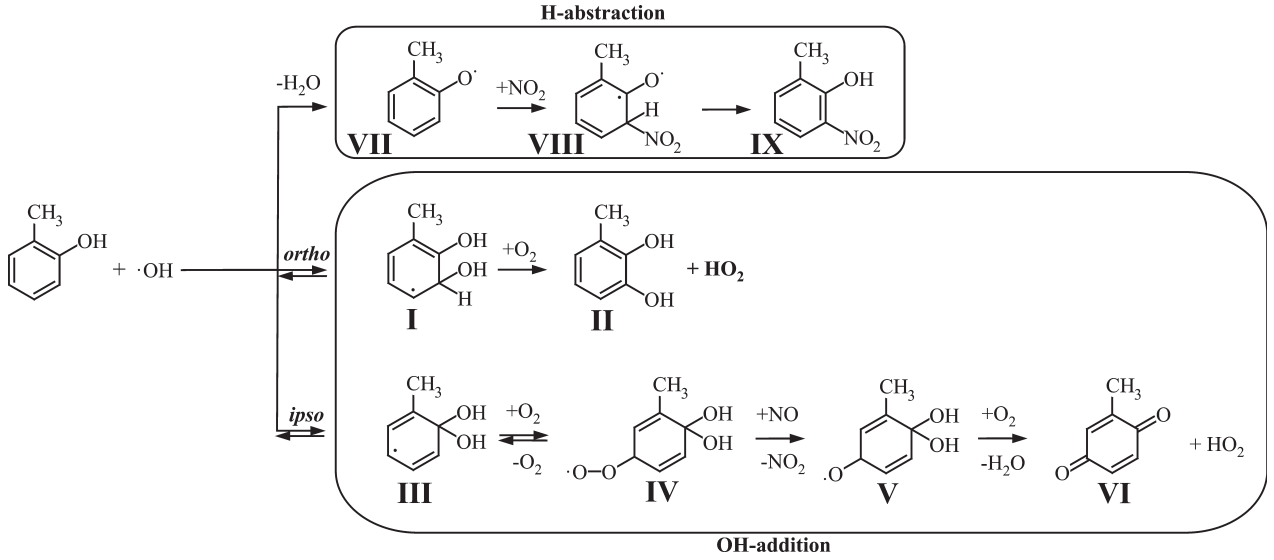


**Figure 2.** Postulated reaction pathways of the OH-initiated oxidation of *o*-cresol.[36,75−77] For convenience, different resonance structures and possible isomers are not shown. $HO_2$ formed without preceding NO reaction steps is indicated in boldface.

longitudinally directed through the reaction volume, with a pulse duration of 10 ns and a fluence of 1.5 mJ $cm^{-2}$ was used for the pulsed photolysis of $O_3$ at 266 nm. Intermediately formed $O(^1D)$ reacted with water vapor to give OH starting concentrations of $\leq 8 \times 10^9$ $cm^{-3}$ formed virtually instantaneously after the 266 nm flash. The photolysis laser beam was expanded to about 3 cm to maximize the irradiated reaction volume. Within the time between two photolysis laser shots (2.5 s), the content of the reaction volume was completely exchanged. Thus, photolysis of reaction products can be excluded as a potential radical source.

The detection of OH radicals was performed 50 cm downstream of the tube inlet by laser-induced fluorescence technique after gas expansion. The air was sampled from the center of the reaction volume through a nozzle (0.2 mm diameter) into a low pressure detection cell operated at 350 Pa. OH fluorescence was induced at 308 nm by use of a tunable frequency-doubled dye laser pumped by a second harmonic of a high repetition rate (8.5 kHz) Nd:YAG laser (Spectra physics, Navigator I). The OH fluorescence emitted from the detection zone was focused onto a gated photomultiplier (Perkin-Elmer, C 1943 P). Photon counts were recorded by a multichannel scaler over a 1 s time interval at a resolution of 5 ms. Sixty decay curves were accumulated to improve the signal-to-noise ratio. Data from the first 10 ms after the photolysis laser flash were discarded because the signal in this interval was unstable. When a small flow of pure NO is added to the expanding gas upstream of the detection zone, $HO_2$ can be partly converted to OH ($HO_2$ + NO → OH + $NO_2$) and detected as additional fluorescence signal ($HO_x$ measurement mode). The $HO_2$ conversion efficiency is limited by the reaction time in the detection cell. Switching between the OH and $HO_x$ measurement modes was possible within a few minutes. OH decay curves were recorded immediately before and after the $HO_x$ decay curves to verify constant experimental conditions, i.e., similar OH starting concentrations and detection sensitivities.

In humidified synthetic air with traces of $O_3$, a background decay rate constant for OH of $k^0_{OH} = 1.5 \pm 0.3$ $s^{-1}$ was observed. The background decay rate constant for $HO_2$ of $k^0_{HO_2} = 1.5 \pm 0.5$ $s^{-1}$ was measured upon addition of CO. Both, $k^0_{OH}$ and $k^0_{HO_2}$ were assigned to diffusion and wall losses. The contribution of the OH + $O_3$ reaction to the OH background decay rate was minor (≈0.1 $s^{-1}$). Radical−radical reactions were estimated unimportant on the basis of typical rate constants of $HO_2$ + $RO_2$ and the $HO_2$ self-reaction.[41]

Besides the secondary formation following reactions of OH, $HO_2$ can also be formed by photolysis of aromatics in the presence of $O_2$. H-atom formation from the 248 nm photolysis of benzene and toluene and subsequent $HO_2$ formation via H + $O_2$ has been observed in previous studies.[42−44] We performed test experiments in the absence of the OH-precursor $O_3$ to check whether H-atoms (and subsequently $HO_2$ radicals) are formed by the 266 nm photolysis of the aromatic hydrocarbons used in this work. For the alkylbenzenes no detectable $HO_2$ formation was observed. In contrast, the 266 nm photolysis of the hydroxybenzenes led to instantaneous $HO_2$ formation. This photolytically produced $HO_2$ was at significant levels compared to the secondarily formed $HO_2$ and was considered quantitatively in the evaluation of experiments with hydroxybenzenes as described below. However, no attempt was made to quantify the $HO_2$ formation in terms of quantum yields for the different compounds.

As reported recently,[40,45] the LIF $HO_2$ detection technique features cross-sensitivity to specific organic peroxy radicals ($RO_2$). This cross-sensitivity is caused by the conversion of $RO_2$ to organic alkoxy radicals (RO) by NO in the LIF detection cell. In contrast to, for example, $CH_3O$, more complex RO can undergo fast decomposition into fragments rapidly forming $HO_2$ in the presence of $O_2$. This applies to α-hydroxy RO from OH + alkene reactions but also to RO from OH + aromatics reactions, e.g., the products of the bicyclic species H in Figure 1. The potential for an additional LIF signal caused by conversion of $RO_2$ to $HO_2$ decreases with decreasing NO concentration in the LIF detection cell. Therefore, the NO concentration in the detection cell was varied over a wide range to quantify and finally widely avoid any $RO_2$ cross-sensitivity.

## MATERIALS

Synthetic air was made from highly purified (99.9999%) liquid samples of $N_2$ and $O_2$. To premix water vapor, the gas flow passed

a saturator filled with pure water (Milli-Q). The aromatic compounds were used as purchased and had stated purities as follows: Toluene (Merck, 99.9%), ethylbenzene (Fluka, 99.0%), *o*-xylene (Fluka, 99.5%), *m*-xylene (Fluka, 99.5%), *p*-xylene (BDH Prolabo, 99.8%), 1,2,3-trimethylbenzene (1,2,3-TMB, LGC, 91.7%), 1,2,4-TMB (LGC, 99.7%), 1,3,5-TMB (Sigma Aldrich, 99.0%), hexamethylbenzene (HMB, Alfa Aesar, 99.0%), phenol (Merck, 99.0%), *o*-cresol (Sigma Aldrich, 99.0%), 2,5-dimethylphenol (Merck, 98.0%), and 2,4,6-trimethylphenol (Acros Organics, 99.0%). Microliter amounts of toluene, ethylbenzene, the xylenes, the trimethylbenzenes, and *o*-cresol were injected into silcosteel containers and pressurized to 330 kPa with nitrogen. The gas mixture from the silcosteel container was then introduced with a mass flow controller to the main gas flow. Milligram amounts of HMB, phenol, 2,5-dimethylphenol, and 2,4,6-trimethylphenol were stored in temperature-controlled flasks that were continuously flushed by a small flow of pure nitrogen. The nitrogen flux was regulated by a mass flow controller and finally introduced to the main gas flow. The concentration of the respective aromatic was estimated from the measured OH reactivity. A 1% mixture of CO in nitrogen was used for experiments, when CO was added (Messer Griesheim, 99.997%). A 10% mixture of NO (Linde, 99.5%) in nitrogen, used for the conversion of $HO_2$ to OH in the detection cell, passed a cartridge filled with sodium hydroxide coated silicate (Ascerite, Sigma-Aldrich) to remove impurities.

## RESULTS

**Data Evaluation.** We alternately measured OH and $HO_x$ decay curves in the presence of aromatic hydrocarbons and extracted prompt $HO_2$ yields by comparison to CO reference experiments. The determination of $HO_2$ yields was done by applying analytical solutions and curve fitting procedures. This approach was recently developed in our study on the OH + benzene reaction[40] and will be reproduced here briefly and extended to account for additional photolytic $HO_2$ formation.

The OH + CO reaction gives $CO_2$ and H-atoms that are quantitatively converted to $HO_2$ within less than $10^{-6}$ s under the experimental conditions. Therefore, the following overall reaction applies:

$$OH + CO + O_2 \rightarrow HO_2 + CO_2 \quad (R1)$$

All reactants were used in excess over OH, so that pseudo-first-order conditions hold. Thus, OH is expected to decay exponentially whereas $HO_2$ should exhibit a rise-and-fall type biexponential behavior:

$$[OH] = [OH]_0 \times \exp(-k_{OH}^{CO} t) \quad (1)$$

$$[HO_2] = \frac{[OH]_0 (k_{OH}^{CO} - k_{OH}^0)}{k_{OH}^{CO} - k_{HO_2}^0} \times \{\exp(-k_{HO_2}^0 t) - \exp(-k_{OH}^{CO} t)\} \quad (2)$$

$k_{OH}^{CO}$ denotes the total OH reactivity in the presence of CO:

$$k_{OH}^{CO} = k_{OH+CO}[CO] + k_{OH}^0 \quad (3)$$

$k_{OH}^0$ and $k_{HO_2}^0$ are the background loss decay rate constants of OH and $HO_2$, respectively. Note that an $HO_2$ yield of unity for the OH + CO reference reaction is presumed in the time dependence of $HO_2$.

The OH + aromatic hydrocarbon (AH) reactions are treated accordingly.

$$OH + AH + O_2 \rightarrow HO_2 + \text{products} \quad (R2)$$

This approach is justified because also the intermediates formed in the OH + AH reactions react rapidly with $O_2$ compared to the time scale of the experiments, i.e., within about $10^{-3}$ s in the case of toluene and even faster for the other compounds.[23] Consequently, we obtain similar expressions for the time dependence of OH and $HO_2$ for the aromatic hydrocarbon experiments, except for a factor $\phi_{HO_2}^{AH}$ that denotes the unknown yield of prompt $HO_2$ and a second term that accounts for a potential photolytical formation of $HO_2$ (see Experimental Methods).

$$[OH] = [OH]_0 \times \exp(-k_{OH}^{AH} t) \quad (4)$$

$$[HO_2] = \frac{[OH]_0 (k_{OH}^{AH} - k_{OH}^0) \phi_{HO_2}^{AH}}{k_{OH}^{AH} - k_{HO_2}^0} \times \{\exp(-k_{HO_2}^0) - \exp(-k_{OH}^{AH} t)\} + [HO_2]_0 \times \exp(-k_{HO_2}^0 t) \quad (5)$$

Again $k_{OH}^{AH}$ is the total OH reactivity in the presence of the aromatic hydrocarbon:

$$k_{OH}^{AH} = k_{OH+AH}[AH] + k_{OH}^0 \quad (6)$$

In the OH mode of the instrument, the obtained LIF signal is proportional to the OH concentration.

$$S_{OH} \propto [OH] \quad (7)$$

In the $HO_x$ mode of the instrument the signal is given by the sum of the OH signal, the signal from $HO_2$ to OH conversion, and possibly a signal from $RO_2$ to OH conversion.

$$S_{HO_x} \propto f_{OH}([OH] + f_{HO_2}([HO_2] + \alpha_{RO_2}[RO_2])) \quad (8)$$

The lower detection sensitivity of OH in the $HO_x$ mode of the instrument was considered by a factor $f_{OH}$ probably caused by a loss of OH through reaction with NO. Furthermore, the detection sensitivity toward $HO_2$ was typically lower by a factor $f_{HO_2}$ compared to that for OH owing to incomplete $HO_2$ conversion because of the limited reaction time. The last term in eq 8 considers any contribution of interfering $RO_2$ radicals. $\alpha_{RO_2}$ is the ratio of the detection sensitivities of $RO_2$ to $HO_2$ that depends on the NO concentration in the LIF detection cell. The time dependencies for $HO_2$ and $RO_2$ are assumed to be similar because radical−radical reactions are negligible under the employed experimental conditions and background losses are also considered similar. Thus, the $RO_2$ concentration can be replaced by the ratio of $RO_2$ and $HO_2$ yields; i.e., the interference can be accounted for by a simple factor $F_{RO_2} \geq 1$:[40]

$$S_{HO_x} \propto f_{OH}([OH] + f_{HO_2}[HO_2](1 + \alpha_{RO_2}\phi_{RO_2}^{AH}/\phi_{HO_2}^{AH})) = f_{OH}([OH] + f_{HO_2}[HO_2]F_{RO_2}) \quad (9)$$

When the NO concentration was decreased in the LIF detection cell, the $RO_2$ to OH conversion was effectively suppressed and $\alpha_{RO_2}$ ideally approached zero whereas $F_{RO_2}$ approached unity.

The product $F_{RO_2} \times \phi_{HO_2}^{AH} = \Phi^{AH}$ was the experimental observable that was finally determined by fitting eqs 1, 2, 4, and 5 simultaneously to the respective $S_{OH}$ and $S_{HO_x}$ decay curves obtained in the presence of CO and the aromatic hydrocarbon. The fits were performed using a Levenberg−Marquardt least-squares fitting procedure[46] where only $k_{OH}^0 = 1.5\ s^{-1}$

Table 1. Fit Results of $f_{OH}$, $f_{HO_2}$, $k_{OH}^{AH}$, and $\Phi^{AH}$ from Combined CO/Alkylbenzene Experiments in Synthetic Air at Different NO Concentrations $[NO]_D$ in the LIF Detection Cell[a]

| reactant | $[NO]_D/10^{14}$ cm$^{-3}$ | $f_{OH}$ | $f_{HO_2}$ | $k_{OH}^{AH}$/s$^{-1}$ | $\Phi^{AH} = \phi_{HO_2}^{AH} F_{RO_2}$ | $\chi^2$/DOF |
|---|---|---|---|---|---|---|
| toluene | 0.12 | 0.84 | 0.22 | 22.3 | 0.42 ± 0.07 | 1.20 |
| | 0.12 | 0.89 | 0.20 | 72.2 | 0.40 ± 0.13 | 1.23 |
| | 1.2 | 0.85 | 0.63 | 43.8 | 0.45 ± 0.14 | 1.16 |
| | | | | | **0.42 ± 0.11**[b] | |
| | 3.9 | 0.87 | 0.94 | 20.1 | 0.56 ± 0.11 | 1.17 |
| | 9.7 | 0.89 | 1.30 | 17.0 | 0.62 ± 0.10 | 1.21 |
| | 15.0 | 0.81 | 1.46 | 17.9 | 0.77 ± 0.13 | 1.27 |
| ethylbenzene | 0.12 | 0.86 | 0.14 | 17.9 | **0.53 ± 0.10** | 1.17 |
| *o*-xylene | 0.12 | 0.97 | 0.15 | 56.4 | **0.41 ± 0.08** | 1.28 |
| *m*-xylene | 0.12 | 0.95 | 0.18 | 74.5 | **0.27 ± 0.06** | 1.23 |
| *p*-xylene | 0.12 | 0.87 | 0.22 | 25.9 | 0.43 ± 0.06 | 1.20 |
| | 0.12 | 0.85 | 0.19 | 74.1 | 0.42 ± 0.15 | 1.28 |
| | 1.2 | 1.00 | 0.67 | 25.8 | 0.36 ± 0.06 | 1.18 |
| | | | | | **0.40 ± 0.09**[b] | |
| | 3.9 | 0.94 | 1.01 | 25.9 | 0.44 ± 0.09 | 1.15 |
| | 9.7 | 0.91 | 1.34 | 25.0 | 0.58 ± 0.11 | 1.28 |
| | 15. | 0.83 | 1.43 | 25.7 | 0.67 ± 0.16 | 1.31 |
| 1,2,3-TMB | 0.12 | 0.97 | 0.18 | 38.7 | **0.31 ± 0.06** | 1.28 |
| 1,2,4-TMB | 0.12 | 0.95 | 0.17 | 53.3 | **0.37 ± 0.09** | 1.33 |
| 1,3,5-TMB | 0.12 | 0.83 | 0.19 | 64.3 | 0.34 ± 0.10 | 1.17 |
| | 0.12 | 0.93 | 0.21 | 18.2 | 0.37 ± 0.06 | 1.14 |
| | 0.24 | 0.89 | 0.27 | 50.4 | 0.25 ± 0.06 | 1.31 |
| | 1.2 | 0.82 | 0.69 | 65.2 | 0.21 ± 0.08 | 1.19 |
| | | | | | **0.29 ± 0.08**[b] | |
| | 2.7 | 0.85 | 1.19 | 42.7 | 0.31 ± 0.07 | 2.07 |
| | 3.9 | 0.81 | 1.06 | 50.8 | 0.34 ± 0.12 | 1.19 |
| | 9.7 | 0.90 | 1.31 | 48.4 | 0.52 ± 0.19 | 1.38 |
| | 15.0 | 0.85 | 1.46 | 28.5 | 0.67 ± 0.15 | 1.28 |
| HMB | 0.12 | 0.88 | 0.14 | 30.0 | 0.32 ± 0.08 | 1.35 |
| | 0.12 | 0.94 | 0.15 | 17.2 | 0.32 ± 0.09 | 1.24 |
| | 0.39 | 0.99 | 0.21 | 18.7 | 0.33 ± 0.06 | 1.25 |
| | | | | | **0.32 ± 0.08**[b] | |

[a] Results were obtained by fitting eq 1, 2, 4, and 5 to the $S_{OH}$ and $S_{HO_x}$ decay curves. Numbers in bold indicate the prompt $HO_2$ yields at $F_{RO_2} \approx 1$. [b] Mean values and mean errors of measurements at $[NO]_D \leq 1.2 \times 10^{14}$ cm$^{-3}$.

(measured separately) was held fixed as a constraint. The idea behind this procedure can be rationalized as follows: By switching quickly from OH to $HO_x$ measurement modes and from CO to AH reactant, we presumed experimental conditions to be constant; i.e., the proportionality factors in eqs 7 and 8 are the same and thus treated as a single fit parameter for each pair of OH and $HO_x$ decay curves. The $S_{OH}$ and $S_{HO_x}$ obtained in the presence of CO then determine the factors $f_{OH}$ and $f_{HO_2}$ whereas the $S_{OH}$ mainly determine the rate constants $k_{OH}^{CO}$ and $k_{OH}^{AH}$. The $S_{HO_x}$ in the presence of AH finally defines $\Phi^{AH}$, i.e., the yield of prompt $HO_2$. However, because all the fit parameters depend on each other more or less strongly, fitting all curves simultaneously ensures that all available experimental information is considered adequately and consistently by weighting with experimental errors according to Poisson statistics (photon counting). The fit quality was assessed on the basis of the weighted sum of squared residuals $\chi^2$ divided by the degrees of freedom (DOF). DOF corresponds to the number of data points minus the number of fitted parameters and $\chi^2$/DOF should ideally range around unity. The typical values of 1.3 found in this study (see Results) are reasonably close to unity and indicate that the errors of the data points were slightly underestimated.

Error estimates for the fitted $\Phi^{AH}$ were also determined by taking into account the mutual dependencies of the fit parameters. Starting with the fitted values, $\Phi^{AH}$ was gradually increased or decreased and held fixed during the fits until the ratio $\chi^2$/DOF increased by a factor ($\approx 1.03$) taken from a parametrization of values for the $\chi^2$-distribution for the given DOF and a probability of 0.68 ($\approx 1\sigma$-errors). Mean errors were then calculated from lower and upper limits.

**OH + Alkylbenzenes.** Table 1 shows the fit results of combined CO/alkylbenzene experiments. Typical decay curves recorded in the presence of CO and toluene are shown in Figure 3, panels (a) and (b). As outlined above, no $HO_2$ formation from photolysis of alkylbenzenes at 266 nm was observed in experiments without OH. Consequently, $[HO_2]_0$ in eq 5 was set to zero.

To check the influence of interfering $RO_2$ radicals, the NO concentration in the LIF detection cell, $[NO]_D$, was varied over a wide range in experiments with toluene, *p*-xylene, and 1,3,5-TMB.


dx.doi.org/10.1021/jp210946y |J. Phys. Chem. A 2012, 116, 6015–6026

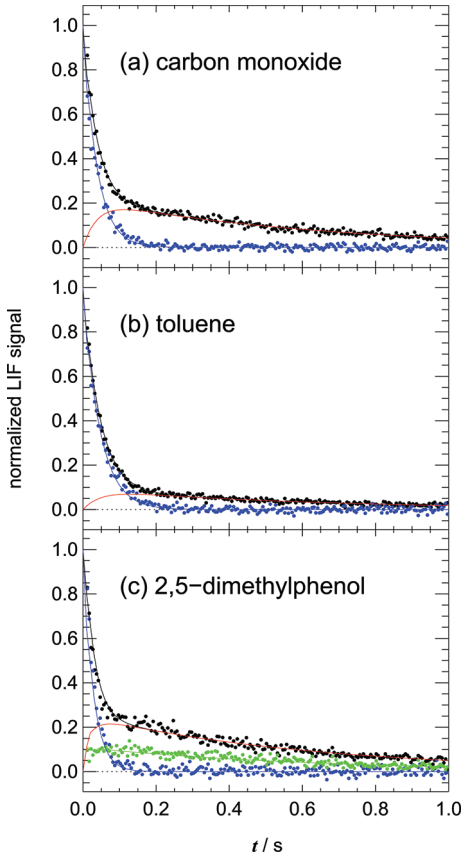


**Figure 3.** Normalized $S_{OH}$ (blue points) and $S_{HO_x}$ (black points) obtained in the presence of CO, toluene, and 2,5-dimethylphenol in synthetic air in the absence of NO in the reaction volume. The NO concentration in the LIF detection cell was $0.12 \times 10^{14}$ cm$^{-3}$ in each experiment (see text). The green points in (c) represent $S_{HO_x}$ obtained in the absence of the OH-precursor ozone. Full lines correspond to fitted decays according to equations eqs 1, 2, 4, and 5. The red lines show the fitted contributions of $HO_2$ to $S_{HO_x}$. The CO experiment in (a) is the corresponding reference experiment for (b). For (c) a similar reference experiment exists but is not shown.

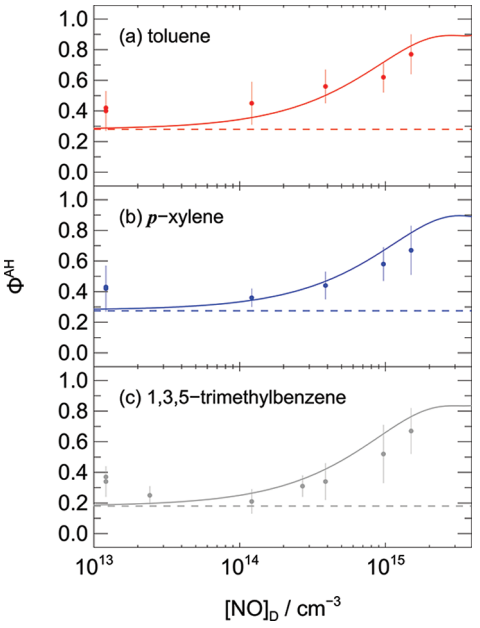


**Figure 4.** Dependence of fitted $\Phi^{AH}$ on $[NO]_D$, the NO concentration in the LIF detection cell. Symbols show results of combined CO/alkylbenzene experiments. The solid lines show the simulated $[NO]_D$ dependence of $\Phi^{AH}$ based on the reactions in Table 2. The dashed lines indicate the presumed contribution of $\phi^{AH}_{HO_2}$ to $\Phi^{AH}$ following the OH + alkylbenzene reaction based on MCM[47,48] recommendations.

**Table 2. Parameters and Rate Constants Used in the Numerical Model to Simulate OH Formation from $HO_2$ and $RO_2$ Radicals in the LIF Detection Cell**

| | |
|---|---|
| reaction time | 250 $\mu$s[a] |
| total pressure | 350 Pa |
| temperature | 298 K |
| $k_{HO_2+NO\rightarrow OH+NO_2}$ | $8.1 \times 10^{-12}$ cm$^3$ s$^{-1}$ [b] |
| $k_{OH+NO\rightarrow HNO_2}$ | $5.7 \times 10^{-14}$ cm$^3$ s$^{-1}$ [b] |
| $k_{OH+NO_2\rightarrow HNO_3}$ | $1.4 \times 10^{-13}$ cm$^3$ s$^{-1}$ [b] |
| $k_{RO_2+NO\rightarrow RO+NO_2}$ | $7.7 \times 10^{-12}$ cm$^3$ s$^{-1}$ [c] |
| $k_{RO_2+NO\rightarrow RNO_3}$ | $1.3 \times 10^{-12}$ cm$^3$ s$^{-1}$ [c] |
| $k_{RO\rightarrow fragments}$ | $1 \times 10^{6}$ s$^{-1}$ [c] |
| $k_{fragments+O_2\rightarrow HO_2}$ | $9.1 \times 10^{-12}$ cm$^3$ s$^{-1}$ [b,d] |

[a] Calculated by fitting the increase of $f_{HO_2}$ with $[NO]_D$.[40] [b] NASA recommendation.[74] [c] MCM recommendation.[47,48] [d] Rate constant assumed similar to $CH_2OH + O_2 \rightarrow HCHO + HO_2$.[74]

As shown in Figure 4, $\Phi^{AH}$ was found to increase with increasing $[NO]_D$, indicating that $RO_2$ radicals contribute significantly to the LIF signal in the $HO_x$ mode at increased $[NO]_D$. Characterization experiments have already been performed for the instrument used in this study[40] and it has been shown that $RO_2$ interferences are sufficiently suppressed using low $[NO]_D$. We performed numerical simulations by taking into account the reactions in the LIF detection cell to reproduce the NO dependencies of the different $\Phi^{AH}$. The full lines in Figure 4 show calculated OH concentrations normalized to a reference case where only $HO_2$ radicals are entering the LIF detection cell. Rate constants and experimental conditions used for the numerical simulations are listed in Table 2. The model was initialized with current recommendations from literature regarding the yields of prompt $HO_2$ and $RO_2$: $\phi^{AH}_{RO_2}/\phi^{AH}_{HO_2} = 0.72/0.28$ for toluene and *p*-xylene and $\phi^{AH}_{RO_2}/\phi^{AH}_{HO_2} = 0.82/0.18$ for 1,3,5-TMB.[47,48] The dotted lines in Figure 4 indicate the recommended prompt $HO_2$ yields and the calculated $\Phi^{AH}$ expectedly approach these limits at decreasing $[NO]_D$, confirming the vanishing influence from peroxy radicals, i.e., $\Phi^{AH} \approx \phi^{AH}_{HO_2}$ at low $[NO]_D$.

The model calculations are in good agreement with the experimental $\Phi^{AH}$ that within experimental uncertainties already leveled out at $[NO]_D \approx 1-2 \times 10^{14}$ cm$^{-3}$. For toluene, *p*-xylene, and 1,3,5-TMB, the final prompt $HO_2$ yields were therefore determined by averaging the results obtained at $[NO]_D \leq 1.2 \times 10^{14}$ cm$^{-3}$ (boldface in Table 1). For the other alkylbenzenes, the full dependence of $\Phi^{AH}$ on $[NO]_D$ was not investigated and most experiments were performed at $[NO]_D = 0.12 \times 10^{14}$ cm$^{-3}$. However, it should be noted that a small, residual $RO_2$ interference ($\alpha_{RO_2} \leq 0.1$) cannot be excluded even at the lowest possible $[NO]_D$ concentrations because of an incomplete understanding of transport processes within the LIF detection cell (e.g., turbulence induced by the gas-expansion and NO mixing effects).[40,45] The prompt $HO_2$ yields determined in this work should therefore be considered upper rather than lower limits.

**OH + Hydroxybenzenes.** The fit results of combined CO/hydroxybenzene experiments are given in Table 3. The experiments

Table 3. Fit Results of $f_{OH}$, $f_{HO_2}$, $k_{OH}^{AH}$, and $\Phi^{AH}$ from Combined CO/Hydroxybenzene Experiments in Synthetic Air at $[NO]_D = 0.12 \times 10^{14}$ cm$^{-3}$ [a]

| reactant | $[HO_2]_0/[OH]_0$ | $f_{OH}$ | $f_{HO_2}$ | $k_{OH}^{AH}/s^{-1}$ | $\Phi^{AH} \approx \phi_{HO_2}^{AH}$ | $\chi^2$/DOF |
|---|---|---|---|---|---|---|
| phenol | 0.33 | 0.88 | 0.33 | 7.9 | 0.89 ± 0.29 | 1.36 |
| | 0.83 | 0.81 | 0.32 | 18.4 | | |
| *o*-cresol | 0.37 | 0.80 | 0.20 | 9.2 | 0.87 ± 0.29 | 1.48 |
| | 0.81 | 0.98 | 0.23 | 17.4 | | |
| 2,5-dimethylphenol | 0.20 | 0.90 | 0.20 | 15.8 | 0.72 ± 0.12 | 1.23 |
| | 0.55 | 1.02 | 0.20 | 38.6 | | |
| 2,4,6-trimethylphenol | 0.01 | 0.93 | 0.19 | 15.8 | 0.45 ± 0.13 | 1.28 |
| | 0.03 | 0.93 | 0.23 | 81.6 | | |

[a] Results were obtained by fitting sets of eqs 1, 2, 4, and 5 to $S_{OH}$ and $S_{HO_x}$ decay curves in the presence of CO and AH. The simultaneous fits cover experiments with two AH concentrations and in the absence of the OH precursor $O_3$ to eliminate the effect of photolytical $HO_2$ formation. Prompt $HO_2$ yields correspond to the measured $\Phi^{AH}$.

revealed that, except for 2,4,6-trimethylphenol, the yields of promptly formed $HO_2$ are much greater than for the alkylbenzenes.

In experiments without the OH-precursor ozone, an instantaneous photolytical $HO_2$ formation was observed as shown in Figure 3c for the example 2,5-dimethylphenol. The same figure also shows $S_{OH}$ and $S_{HO_x}$ curves recorded in the presence of ozone where $S_{HO_x}$ is expected to contain an underlying contribution from photolytically produced $HO_2$. The latter, $[HO_2]_0$ in eq 5, is assumed to depend linearly on the concentration of the aromatic hydrocarbon. In a first approach, measurements were therefore performed at two different AH concentrations and two $S_{OH}$ and $S_{HO_x}$ decay curves each were recorded. Two sets of eqs 1, 2, 4, and 5 were then fitted simultaneously by assuming $[HO_2]_0 \propto [AH]$ treating the proportionality factor as an additional fit parameter. Although this fitting strategy worked technically, the obtained error limits were significantly greater than in the case of the alkylbenzenes and approached 100%. Obviously, the distinction of photolytically and secondarily formed $HO_2$ is difficult, which results in a large mutual dependence of the respective contributions and increased error limits. Therefore, an extended evaluation procedure was adopted where also the decay curves $S_{HO_x}$ obtained in the absence of the OH-precursor ozone were implemented in the fits by setting $[OH]_0 = 0$ in eq 5. This led to similar results with improved error limits as listed in Table 3.

$[NO]_D$ concentrations were always kept low during the experiments with hydroxybenzenes. We therefore again assume $\Phi^{AH} \approx \phi_{HO_2}^{AH}$. Because prompt $HO_2$ yields were greater compared to those of the alkylbenzenes, any residual contribution of $RO_2$ interferences is expected to be even smaller and negligible.

## DISCUSSION

In the experiments outlined above, we determined $HO_2$ yields upon the OH + aromatic hydrocarbon reaction in synthetic air in the absence of NO. These yields are helpful to reduce budget uncertainties regarding the primary oxidation steps because the extracted $\phi_{HO_2}$ should match the combined yields of currently proposed $HO_2$ coproducts. From OH + alkylbenzenes these coproducts are phenols, epoxides, and oxepins (Figure 1):

$$\phi_{HO_2}^{\text{alkylbenzene}} = \phi_{\text{phenol}} + \phi_{\text{epoxide}} + \phi_{\text{oxepin}} \quad (10)$$

From OH + hydroxybenzenes the coproducts are dihydoxybenzenes (Figure 2):

$$\phi_{HO_2}^{\text{hydroxybenzene}} = \phi_{\text{dihydoxybenzene}} \quad (11)$$

On the other hand, the remainder $(1 - \phi_{HO_2})$ should match the combined yields of reaction channels not associated with prompt $HO_2$ formation. From OH + alkylbenzenes, these are the bicyclic peroxy radical channel leading to $\alpha$-dicarbonyls, the H-atom abstraction finally forming benzaldehydes, and the dealkylation (Figure 1):

$$1 - \phi_{HO_2}^{\text{alkylbenzene}} = \phi_{\text{dicarbonyl}} + \phi_{\text{benzaldehyde}} + \phi_{\text{dealkylation}} \quad (12)$$

For OH + hydroxybenzenes $(1 - \phi_{HO_2})$ should match the yield of nitrophenols from the H-atom abstraction channel plus the yield of 1,4-benzoquinones formed following the proposed *ipso*-OH-addition (Figure 2):

$$1 - \phi_{HO_2}^{\text{hydroxybenzene}} = \phi_{\text{nitrophenol}} + \phi_{\text{quinone}} \quad (13)$$

**OH + Toluene and Ethylbenzene.** For the OH + toluene reaction we determined $\phi_{HO_2}^{\text{toluene}} = 0.42 \pm 0.11$. This yield is significantly greater than the $\phi_{\text{phenol}}$ (i.e., cresol) yield of 0.18−0.28 reported in most product studies[14,25,27,31,49,50] (Table 4). Exceptions are considerably greater and smaller values from two studies[51,52] that are supposed not to be representative for atmospheric conditions because of potential influence of heterogeneous reactions[51] or due to losses of primary oxidation products upon reaction with OH.[52] The result of our study is consistent with the currently proposed toluene degradation mechanism where the coproducts of prompt $HO_2$ are cresols and an epoxide. By comparison of $\phi_{HO_2}^{\text{toluene}}$ to the reported cresol yields, formation of 0.14−0.24 of other $HO_2$ coproducts is possible. Flowtube studies by Baltaretu et al.[27] and Birdsall et al.[31] indeed reported experimental evidence for the epoxide pathway. The combined yield of cresol and epoxide of 0.35 ± 0.07[27] is similar to $\phi_{HO_2}^{\text{toluene}}$ determined in this work. Bloss et al.[48] estimated a combined yield of 0.28 for cresol and epoxide based on the data by Volkamer et al.[33] to close the budget for the OH-initiated degradation of toluene. This value is somewhat lower than the result of our study. Owing to the uncertainties of the primary product yields, it cannot be ruled out that there are further reaction channels yielding prompt $HO_2$ like the oxepin pathway proposed by Klotz et al.[53−55] This reaction channel has so far only been excluded for OH + benzene.[35]

The remainder $(1 - \phi_{HO_2}^{\text{toluene}}) = 0.58 \pm 0.11$ is also somewhat greater than the combined yields $\phi_{\text{dicarbonyl}} + \phi_{\text{benzaldehyde}}$ determined in product studies: 0.47 ± 0.03,[25] 0.39 ± 0.10,[33] and 0.35 ± 0.10.[27] This discrepancy can be attributed to the great


dx.doi.org/10.1021/jp210946y | J. Phys. Chem. A 2012, 116, 6015–6026

Table 4. Product Yields of the OH-Initiated Oxidation of Toluene in the Presence of $O_2$ from Literature

| reference | prompt $HO_2$ reaction channels | | reaction channels not associated with prompt $HO_2$ | | | experimental conditions |
|---|---|---|---|---|---|---|
| | $\phi_{phenol}$ [a] | $\phi_{epoxide}$ [b] | $\phi_{dicarbonyl}$ | $\phi_{benzaldehyde}$ | $\phi_{dealkylation}$ [c] | |
| | | | OH + Toluene | | | |
| Atkinson et al.[49] | 0.25 ± 0.03 | | | 0.07 ± 0.01 | | ≈15 ppm $NO_x$ |
| Seuwen et al.[51] | 0.53 ± 0.08[d] | | 0.10 ± 0.02[e] | 0.05 ± 0.01 | | $NO_x$-free |
| Smith et al.[25] | 0.18 ± 0.01 | | 0.41 ± 0.03[e] | 0.06 ± 0.01 | | <1 ppm $NO_x$ |
| Klotz et al.[50] | 0.18 ± 0.03 | | | 0.06 ± 0.01 | | 3−300 ppb $NO_x$ |
| Moschonas et al.[52] | 0.09 ± 0.03 | | | 0.08 ± 0.01 | | $NO_x$-free |
| Volkamer et al.[33] | | | 0.39 ± 0.10[f] | | | <1 ppm $NO_x$ |
| Noda et al.[14] | 0.18 ± 0.02 | | | | 0.05 ± 0.01 | 0.01−0.1 ppm $NO_x$ |
| Baltaretu et al.[27] | 0.28 ± 0.06 | 0.07 ± 0.03 | 0.30 ± 0.10[e,g] | 0.05 ± 0.02 | | $NO_x$-free |
| Birdsall et al.[31] | ≈0.22[h] | ≈0.05[h] | | ≈0.07[h] | ≈0.07[h] | $NO_x$-free |
| Nishino et al.[67] | | | 0.48 ± 0.03[e] | | | 0.08−4 ppm $NO_x$ |
| this study | $\phi_{HO_2} = 0.42 \pm 0.11$ | | | $(1 - \phi_{HO_2}) = 0.58 \pm 0.11$ | | $NO_x$-free |

[a] Sum of *o*-, *m*-, and *p*-cresol. [b] 2-Methyl-2,3-epoxy-6-oxo-4-hexenal. [c] Phenol. [d] Sum of *o*- and *p*-cresol. [e] Sum of glyoxal and methylglyoxal. [f] Glyoxal. [g] Prediction for α-dicarbonyl formation upon a second OH attack. [h] Relative product yield.

uncertainty of $\phi_{dicarbonyl}$ and to missing minor (<0.10)[14,31] reaction channels like the dealkylation pathway that was experimentally confirmed in flowtube studies by Noda et al.[14] and Birdsall et al.[31]

For the OH + ethylbenzene reaction we determined $\phi_{HO_2}^{ethylbenzene} = 0.53 \pm 0.10$. Only a few experimental studies on the photo-oxidation of ethylbenzene are available in literature.[56−59] These studies focused on the formation of secondary organic aerosol and no quantitative information about gaseous oxidation products was reported. However, the $HO_2$ coproduct ethylphenol was found to be a major oxidation product.[56,59] Owing to the lack of absolute product yields, we are not able to draw further conclusions concerning other reaction channels yielding prompt $HO_2$.

**OH + Isomeric Xylenes.** In the case of *o*-xylene and *p*-xylene we obtained prompt $HO_2$ yields of 0.41 ± 0.08 and 0.40 ± 0.09, respectively. The formation yields of the corresponding dimethylphenols were reported to be 0.10−0.16[14,60,61] and 0.12−0.19,[14,26,61−63] respectively (Table 5). Again, our results suggest that non-phenol reaction pathways, e.g., epoxide formation, contribute significantly (<0.30) to the prompt $HO_2$ formation, which is consistent with the current understanding of the xylene degradation mechanism. For OH + *o*-xylene our result is in line with the estimation by Bloss et al.[48] for $(\phi_{phenol} + \phi_{epoxide}) = 0.40$. For OH + *p*-xylene the estimation is somewhat lower: $(\phi_{phenol} + \phi_{epoxide}) = 0.28$.[48] To date, there is no quantitative information on the formation of epoxide compounds from *o*- and *p*-xylene but species with corresponding molecular weights have been observed.[28,29,64]

The remainders of $(1 - \phi_{HO_2}^{o\text{-xylene}}) = 0.59 \pm 0.08$ and $(1 - \phi_{HO_2}^{p\text{-xylene}}) = 0.60 \pm 0.09$ determined in this work are in reasonable agreement with $\phi_{dicarbonyl} + \phi_{benzaldehyde}$ reported in several studies: 0.40−0.60[65−67] for *o*-xylene and 0.40−0.70[26,62,63,65−67] for *p*-xylene (Table 5). The uncertainties of the reported product yields leave some scope for additional minor reaction pathways like the dealkylation postulated by Noda et al.: $\phi_{dealkylation}$ = 0.04−0.05.[14]

For *m*-xylene the situation is different because the gap between $\phi_{HO_2}^{m\text{-xylene}} = 0.27 \pm 0.06$ and $\phi_{phenol}$ (i.e., dimethylphenol) from product studies of 0.11−0.21[14,26,30,60,61] is smaller than for *o*- and *p*-xylene. Moreover, in a recent study by Zhao et al.[30] the formation of epoxides from *m*-xylene with a yield of ≈0.02 was reported for the first time. The combined yield of $(\phi_{phenol} + \phi_{epoxide}) = 0.19 \pm 0.03$[30] corresponds quite well to the prompt $HO_2$ yield determined in this work. Accordingly, $HO_2$ formation via the epoxide reaction channel is considered to be of minor importance for *m*-xylene. Most of the previous product studies on *m*-xylene reported combined formation yields of $\phi_{dicarbonyl} + \phi_{benzaldehyde}$ ranging between 0.40 and 0.60.[26,65−67] Zhao et al. reported a considerably lower value of 0.21.[30] The authors attributed this discrepancy mainly to their very low yield of methylglyoxal (0.15) obtained in a fast turbulent flow reactor. When the remainder of $(1 - \phi_{HO_2}^{m\text{-xylene}}) = 0.73 \pm 0.06$ is compared to these literature values of $\phi_{dicarbonyl} + \phi_{benzaldehyde}$, it becomes obvious that the carbon balance is not closed. Taking into account the data by Bandow et al.,[65] Smith et al.,[26] Arey et al.,[66] and Nishino et al.,[67] 0.10−0.30 of the primary oxidation products not associated with prompt $HO_2$ are not identified so far. This gap can at least partly be closed by the dealkylation pathway yielding cresol reported by Noda et al.:[14] $\phi_{dealkylation} = 0.11 \pm 0.04$. Contradictory results were reported by Aschmann et al.[15] who determined a cresol yield of <0.02 for *m*-xylene and suggested that the ion peaks observed by Noda et al.[14] could correspond to the sum of cresol and methyloxepin (both resulting from dealkylation and having the same mass-to-charge-ratio). A corresponding dealkylation mechanism yielding methyloxepin following the OH + *m*-xylene reaction was postulated.[14,15]

**OH + Isomeric Trimethylbenzenes.** The $HO_2$ yields of the OH + TMB reactions were determined to be 0.31 ± 0.06 (1,2,3-TMB), 0.37 ± 0.09 (1,2,4-TMB), and 0.29 ± 0.08 (1,3,5-TMB). Only a few product studies[26,63,68,69] reported the formation of phenols from TMB photo-oxidation. Quantitative information was only given by Smith et al.[26] and Volkamer[63] (phenol yields ≤0.07, see Table 6). Formation of epoxide compounds has not yet been observed. Nevertheless, Bloss et al.[48] assigned epoxide yields of 0.21 (1,2,3-TMB), 0.30 (1,2,4-TMB), and 0.14 (1,3,5-TMB) to close the carbon balance. Our result support the recommendations given by Bloss et al.[48] However, we merely conclude that non-phenol reaction channels contribute significantly to prompt $HO_2$ formation (<0.30).

**Table 5. Product Yields of the OH-Initiated Oxidation of the Isomeric Xylenes in the Presence of $O_2$ from Literature**

| | prompt $HO_2$ reaction channels | | reaction channels not associated with prompt $HO_2$ | | | |
|---|---|---|---|---|---|---|
| reference | $\phi_{phenol}$ [a] | $\phi_{epoxide}$ [b] | $\phi_{dicarbonyl}$ | $\phi_{benzaldehyde}$ [c] | $\phi_{dealkylation}$ [d] | experimental conditions |
| | | | OH + *o*-Xylene | | | |
| Bandow et al.[65] | | | 0.41 ± 0.04[e] | 0.05 ± 0.01 | | 2 ppm $NO_x$ |
| Gery et al.[60] | 0.10 ± 0.04 | | | 0.17 ± 0.07 | | ≈8 ppm $NO_x$ |
| Atkinson et al.[61] | 0.16 ± 0.02 | | | 0.05 ± 0.01 | | 1−13 ppm $NO_2$ |
| Arey et al.[66] | | | 0.61[e] | | | <1 ppm $NO_x$ |
| Noda et al.[14] | 0.11 ± 0.05 | | | | 0.05 ± 0.03 | 0.01−0.1 ppm $NO_x$ |
| Nishino et al.[67] | | | 0.46 ± 0.06[f] | | | 0.08−4 ppm $NO_x$ |
| this study | $\phi_{HO_2} = 0.41 \pm 0.08$ | | $(1 - \phi_{HO_2}) = 0.59 \pm 0.08$ | | | $NO_x$-free |
| | | | OH + *m*-Xylene | | | |
| Bandow et al.[65] | | | 0.55 ± 0.07[f] | 0.04 ± 0.01 | | 2 ppm $NO_x$ |
| Gery et al.[60] | 0.18 ± 0.07 | | | 0.13 ± 0.06 | | ≈8 ppm $NO_x$ |
| Atkinson et al.[61] | 0.21 ± 0.03[j] | | | 0.03 ± 0.01 | | 0−10 ppm $NO_2$ |
| Smith et al.[26] | 0.11 ± 0.01 | | 0.48 ± 0.02[f] | 0.05 ± 0.01 | | <1 ppm $NO_x$ |
| Zhao et al.[30] | 0.17 ± 0.03[j] | 0.02 ± 0.01 | 0.15 ± 0.04[g] | 0.06 ± 0.01 | | ≈0.3 ppm $NO_x$ |
| Arey et al.[66] | | | 0.46[f] | | | <1 ppm $NO_x$ |
| Noda et al.[14] | 0.14 ± 0.03 | | | | 0.11 ± 0.04 | 0.01−0.1 ppm $NO_x$ |
| Aschmann et al.[15] | | | | | <0.02 | <20 ppm $NO_x$ |
| Nishino et al.[67] | | | 0.63 ± 0.09[f] | | | 0.08−4 ppm $NO_x$ |
| this study | $\phi_{HO_2} = 0.27 \pm 0.06$ | | $(1 - \phi_{HO_2}) = 0.73 \pm 0.06$ | | | $NO_x$-free |
| | | | OH + *p*-Xylene | | | |
| Bandow et al.[65] | | | 0.36 ± 0.03[f] | 0.08 ± 0.01 | | 2 ppm $NO_x$ |
| Atkinson et al.[61] | 0.19 ± 0.04 | | | 0.07 ± 0.01 | | 1−10 ppm $NO_2$ |
| Smith et al.[26] | 0.13 ± 0.02 | | 0.61 ± 0.11[f] | 0.10 ± 0.02 | | <1 ppm $NO_x$ |
| Bethel et al.[62] | 0.14 ± 0.02 | | (0.32[i]) | 0.07 ± 0.01 | | 0.8−3.3 ppm $NO_x$ |
| Volkamer et al.[33] | | | 0.40 ± 0.11[h] | | | <1 ppm $NO_x$ |
| Volkamer et al.[63] | 0.12 ± 0.03 | | | 0.08 ± 0.02 | | <1 ppm $NO_x$ |
| Arey et al.[66] | | | 0.49[f] | | | <1 ppm $NO_x$ |
| Noda et al.[14] | 0.13 ± 0.03 | | | | 0.04 ± 0.03 | 0.01−0.1 ppm $NO_x$ |
| Nishino et al.[67] | | | 0.58 ± 0.05[f] | | | 0.08−4 ppm $NO_x$ |
| this study | $\phi_{HO_2} = 0.40 \pm 0.09$ | | $(1 - \phi_{HO_2}) = 0.60 \pm 0.09$ | | | $NO_x$-free |

[a] Primary phenol products: from *o*-xylene, (2,3 + 3,4)-dimethylphenol; from *m*-xylene, (2,4 + 2,6 + 3,5)-dimethylphenol; from *p*-xylene, 2,5-dimethylphenol. [b] Sum of 2,4-dimethyl-2,3-epoxy-6-oxo-4-hexenal, 2,6-dimethyl-2,3-epoxy-6-oxo-4-hexenal, and 3,5-dimethyl-2-hydroxyl-3,4-epoxy-5-hexenal. [c] Primary substituted benzaldehyde products: from *o*-xylene, 2-methylbenzaldehyde; from *m*-xylene, 3-methylbenzaldehyde; from *p*-xylene, 4-methylbenzaldehyde. [d] Cresol. [e] Sum of glyoxal, methylglyoxal, and dimethylglyoxal. [f] Sum of glyoxal and methylglyoxal. [g] Methylglyoxal. [h] Glyoxal. [i] 3-Hexene-2,5-dione; extrapolated to $NO_x$-free conditions. [j] Sum of 2,4- and 2,6-dimethylphenol.

For the reaction channels not associated with prompt $HO_2$ we derived $(1 - \phi_{HO_2}) = 0.69 \pm 0.06$ (1,2,3-TMB), $0.63 \pm 0.09$ (1,2,4-TMB), and $0.71 \pm 0.08$ (1,3,5-TMB). These results are similar to $(\phi_{dicarbonyl} + \phi_{benzaldehyde}) = 0.40-0.70$ determined in previous studies.[26,62,66,67,70] Lower values for $\phi_{dicarbonyl}$ of $0.20 \pm 0.03$ (1,2,3-TMB) and $0.36 \pm 0.08$ (1,2,4-TMB) were determined by Nishino et al.[67] because dimethylglyoxal was not measured. A single exception is the work by Smith et al.[26] who obtained $(\phi_{dicarbonyl} + \phi_{benzaldehyde}) = 0.93 \pm 0.25$ for the OH + 1,3,5-TMB reaction. This is somewhat greater than $1 - \phi_{HO_2}^{1,3,5\text{-TMB}}$ determined in our study but still in agreement within the combined errors. The dealkylation pathway may be operative for the OH + TMB reaction but is probably of minor (<0.10) importance.

**OH + Hexamethylbenzene.** The OH + HMB reaction gave $\phi_{HO_2}^{HMB} = 0.32 \pm 0.08$. No product studies on the photo-oxidation of HMB are available. Only a single flowtube study by Berndt and Böge[71] performed at 295 K and 25 mbar in He reported the formation of hexamethyl-2,4-cyclohexadienone following the OH + HMB reaction in the presence of $NO_2$. Assuming a similar HMB oxidation mechanism in the presence of $O_2$, hexamethyl-2,4-cyclohexadienone could be the coproduct of prompt $HO_2$. However, no experimental evidence for this reaction is available so far.

**OH + Hydroxybenzenes.** The prompt $HO_2$ yields extracted from the OH + hydroxybenzene experiments, $\phi_{HO_2}^{phenol} = 0.89 \pm 0.29$, $\phi_{HO_2}^{o\text{-cresol}} = 0.87 \pm 0.29$, and $\phi_{HO_2}^{2,5\text{-dimethylphenol}} = 0.72 \pm 0.12$, are considerably greater compared to those from alkylbenzenes with the exception of $\phi_{HO_2}^{2,4,6\text{-trimethylphenol}} = 0.45 \pm 0.13$. Our results are consistent with previous product studies reporting high dihydroxybenzene yields of 0.7−0.8[36,72,73] from OH + phenol and OH + *o*-cresol (Table 7). This confirms that $HO_2$ is formed as coproduct of dihydoxybenzenes.

The contributions of reaction channels not associated with prompt $HO_2$ were determined to be $(1 - \phi_{HO_2}^{phenol}) = 0.11 \pm 0.29$

**Table 6. Product Yields of the OH-Initiated Oxidation of the Isomeric Trimethylbenzenes in the Presence of $O_2$ from Literature**

| | prompt $HO_2$ reaction channels | reaction channels not associated with prompt $HO_2$ | | |
|---|---|---|---|---|
| reference | $\phi_{phenol}$ [a] | $\phi_{dicarbonyl}$ | $\phi_{benzaldehyde}$ [b] | experimental conditions |
| | | OH + 1,2,3-TMB | | |
| Bandow et al.[70] | | 0.70 ± 0.02[c] | | 2 ppm $NO_x$ |
| Bethel et al.[62] | | 0.52[f] | | 0.8−3.3 ppm $NO_x$ |
| Arey et al.[66] | | 0.59[c] | | <1 ppm $NO_x$ |
| Nishino et al.[67] | | 0.20 ± 0.03[d] | | 0.08−4 ppm $NO_x$ |
| this study | $\phi_{HO_2}$ = 0.31 ± 0.06 | $(1-\phi_{HO_2})$ = 0.69 ± 0.06 | | $NO_x$-free |
| | | OH + 1,2,4-TMB | | |
| Bandow et al.[70] | | 0.56 ± 0.02[c] | | 2 ppm $NO_x$ |
| Smith et al.[26] | 0.02 ± 0.01 | 0.62 ± 0.07[c] | 0.04 ± 0.01 | <1 ppm $NO_x$ |
| Bethel et al.[62] | | 0.41[g] | | 0.8−3.3 ppm $NO_x$ |
| Arey et al.[66] | | 0.50[c] | | <1 ppm $NO_x$ |
| Nishino et al.[67] | | 0.36 ± 0.08[d] | | 0.08−4 ppm $NO_x$ |
| this study | $\phi_{HO_2}$ = 0.37 ± 0.09 | $(1-\phi_{HO_2})$ = 0.63 ± 0.09 | | $NO_x$-free |
| | | OH + 1,3,5-TMB | | |
| Bandow et al.[70] | | 0.64 ± 0.03[e] | | 2 ppm $NO_x$ |
| Smith et al.[26] | 0.04 ± 0.01 | 0.90 ± 0.25[e] | 0.03 ± 0.01 | <1 ppm $NO_x$ |
| Volkamer et al.[63] | 0.07 ± 0.01 | | 0.03 ± 0.01 | <5 ppm $NO_x$ |
| Arey et al.[66] | | 0.60[e] | | <1 ppm $NO_x$ |
| Nishino et al.[67] | | 0.58 ± 0.05[e] | | 0.08−4 ppm $NO_x$ |
| this study | $\phi_{HO_2}$ = 0.29 ± 0.08 | $(1-\phi_{HO_2})$ = 0.71 ± 0.08 | | $NO_x$-free |

[a] Primary phenol products: from 1,2,4-TMB, (2,3,5 + 2,3,6 + 2,4,5)-trimethylphenol; from 1,3,5-TMB, 2,4,6-trimethylphenol. [b] Primary substituted benzaldehyde products: from 1,2,4-TMB, (2,4 + 3,4 + 2,5)-dimethylbenzaldehyde; from 1,3,5-TMB, 3,5-dimethylbenzaldehyd. [c] Sum of glyoxal, methylglyoxal, and dimethylglyoxal. [d] Sum of glyoxal and methylglyoxal. [e] Methylglyoxal. [f] Dimethylglyoxal; extrapolated to $NO_x$-free conditions [g] Sum of dimethylglyoxal and 3-hexene-2,5-dione; extrapolated to $NO_x$-free conditions.

**Table 7. Product Yields of the OH-Initiated Oxidation of Phenol and *o*-Cresol in the Presence of $O_2$ from Literature**

| | prompt $HO_2$ reaction channel | reaction channels not associated with promt $HO_2$ | | |
|---|---|---|---|---|
| reference | $\phi_{dihydroxbenzene}$ [a] | $\phi_{nitrophenol}$ [b] | $\phi_{quinone}$ [c] | experimental conditions |
| | | OH + Phenol | | |
| Olariu et al.[36] | 0.80 ± 0.12 | 0.06 ± 0.01 | 0.04 ± 0.01 | <2 ppn NO |
| Berndt et al.[72] | 0.73 ± 0.04 | 0.04 ± 0.02 | 0.01 ± 0.01 | 4−100 ppm NO |
| This study | $\phi_{HO_2}$ = 0.89 ± 0.29 | $(1-\phi_{HO_2})$ = 0.11 ± 0.29 | | $NO_x$-free |
| | | OH + *o*-Cresol | | |
| Olariu et al.[36] | 0.73 ± 0.15 | 0.07 ± 0.02 | 0.07 ± 0.02 | <2 ppm NO |
| Coeur-Tourneur et al.[73] | | 0.05 ± 0.01 | 0.06 ± 0.01 | 1.3−1.5 ppm NO |
| this study | $\phi_{HO_2}$ = 0.87 ± 0.29 | $(1-\phi_{HO_2})$ = 0.13 ± 0.29 | | $NO_x$-free |

[a] Primary dihydroxybenzene products: from phenol, 1,2-dihydroxybenzene; from *o*-cresol, 3-methyl-1,2-dihydoxybenzene. [b] Primary nitrophenol products: from phenol, 2-nitrophenol; from *o*-cresol, 6-methyl-2-nitrophenol. [c] Primary quinone products: from phenol, 1,4-benzoquinone; from *o*-cresol, methyl-1,4-benzoquinone.

and $(1-\phi_{HO_2}^{o\text{-cresol}}) = 0.13 \pm 0.29$. Although the errors are considerable, these yields correspond well to reported $\phi_{nitrophenol} + \phi_{quinone}$ from phenol (0.10 ± 0.02)[36] and *o*-cresol (0.14 ± 0.04),[36] respectively. No product studies are available in literature for 2,5-dimethylphenol and 2,4,6-trimethylphenol.

## CONCLUSIONS

We determined yields of promptly formed $HO_2$ ($\phi_{HO_2}$) following the reaction of OH with selected aromatic hydrocarbons under atmospheric conditions. This experimental approach is complementary to previous product studies and can help to reduce budget uncertainties concerning the initial reaction steps of the OH-initiated atmospheric photo-oxidation of aromatics. Our results suggest that for most of the investigated alkylbenzenes (with the exception of *m*-xylene) a significant fraction of prompt $HO_2$ is formed via pathways not forming phenols (e.g., formation of epoxides or oxepins). The remainder $(1-\phi_{HO_2})$ revealed that, besides the established H-atom abstraction and bicyclic peroxy radical pathways, minor non-$HO_2$ forming

reaction channels (e.g., dealkylation) remain possible for all investigated alkylbenzenes. The investigated hydroxybenzenes (phenol, *o*-cresol, 2,5-dimethylphenol, 2,4,6-trimethylphenol) are also forming prompt $HO_2$ with high yields. In the case of OH + phenol and OH + *o*-cresol, the results are consistent with $HO_2$ being exclusively formed as coproduct of dihydroxybenzenes.

## AUTHOR INFORMATION


### Corresponding Author

*E-mail: b.bohn@fz-juelich.de.


## ACKNOWLEDGMENT

We thank M. Bachner, H. Fuchs, A. Hofzumahaus, F. Holland, and S. Lou for useful discussions and technical support. S.N. thanks the Deutsche Forschungsgemeinschaft for a Ph.D. studentship under grant BO 1580/3-1.

## REFERENCES


(1) Fortin, T. J.; Howard, B. J.; Parrish, D. D.; Goldan, P. D.; Kuster, W. C.; Atlas, E. L.; Harley, R. A. *Environ. Sci. Technol.* **2005**, *39*, 1403–1408.

(2) Ilgen, E.; Karfich, N.; Levsen, K.; Angerer, J.; Schneider, P.; Heinrich, J.; Wichmann, H.; Dunemann, L.; Begerow, J. *Atmos. Environ.* **2001**, *35*, 1235–1252.

(3) Ilgen, E.; Levsen, K.; Angerer, J.; Schneider, P.; Heinrich, J.; Wichmann, H. *Atmos. Environ.* **2001**, *35*, 1253–1264.

(4) Ilgen, E.; Levsen, K.; Angerer, J.; Schneider, P.; Heinrich, J.; Wichmann, H. *Atmos. Environ.* **2001**, *35*, 1265–1279.

(5) Johnson, M. M.; Williams, R.; Fan, Z.; Lin, L.; Hudgens, E.; Gallagher, J.; Vette, A.; Neas, L.; Ozkaynak, H. *Atmos. Environ.* **2010**, *44*, 4927–4936.

(6) Hawthorne, S.; Miller, D.; Barkley, R.; Krieger, M. *Environ. Sci. Technol.* **1988**, *22*, 1191–1196.

(7) Hawthorne, S.; Miller, D.; Langenfeld, J.; Krieger, M. *Environ. Sci. Technol.* **1992**, *26*, 2251–2262.

(8) U.S. Environmental Protection Agency, Our Nation's Air (EPA-454/R-09-002), 2010.

(9) Atkinson, R.; Arey, J. *Polycyclic Aromatic Compounds* **2007**, *27*, 15–40.

(10) Calvert, J. G.; Atkinson, R.; Becker, K. H.; Kamens, R. M.;Seinfeld, J. H.; Wallington, T. J.; Yarwood, G. *Mechanisms of atmospheric oxidation of aromatic hydrocarbons*; Oxford University Press: Oxford, U.K., 2002.

(11) Atkinson, R.; Arey, J. *Chem. Rev.* **2003**, *103*, 4605–4638.

(12) Ravishankara, A.; Wagner, S.; Fischer, S.; Smith, G.; Schiff, R.; Watson, R.; Tesi, G.; Davis, D. *Int. J. Chem. Kinet.* **1978**, *10*, 783–804.

(13) Warneke, C.; et al. *J. Geophys. Res.-Atmos.* **2004**, *109*, D10309.

(14) Noda, J.; Volkamer, R.; Molina, M. J. *J. Phys. Chem. A* **2009**, *113*, 9658–9666.

(15) Aschmann, S. M.; Arey, J.; Atkinson, R. *Atmos. Environ.* **2010**, *44*, 3970–3975.

(16) Wahner, A.; Zetzsch, C. *J. Phys. Chem.* **1983**, *87*, 4945–4951.

(17) Witte, F.; Urbanik, E.; Zetzsch, C. *J. Phys. Chem.* **1986**, *90*, 3251–3259.

(18) Knispel, R.; Koch, R.; Siese, M.; Zetzsch, C. *Ber. Bunsen-Ges.* **1990**, *94*, 1375–1379.

(19) Bohn, B.; Zetzsch, C. *Phys. Chem. Chem. Phys.* **1999**, *1*, 5097–5107.

(20) Bohn, B. *J. Phys. Chem. A* **2001**, *105*, 6092–6101.

(21) Grebenkin, S.; Krasnoperov, L. *J. Phys. Chem. A* **2004**, *108*, 1953–1963.

(22) Raoult, S.; Rayez, M. T.; Rayez, J. C.; Lesclaux, R. *Phys. Chem. Chem. Phys.* **2004**, *6*, 2245–2253.

(23) Koch, R.; Knispel, R.; Elend, M.; Siese, M.; Zetzsch, C. *Atmos. Chem. Phys.* **2007**, *7*, 2057–2071.

(24) Atkinson, R.; Baulch, D.; Cox, R.; Hampson, R.; Kerr, J.; Troe, J. *J. Phys. Chem. Ref. Data* **1989**, *18*, 881–1097.

(25) Smith, D.; McIver, C.; Kleindienst, T. *J. Atmos. Chem.* **1998**, *30*, 209–228.

(26) Smith, D.; Kleindienst, T.; McIver, C. *J. Atmos. Chem.* **1999**, *34*, 339–364.

(27) Baltaretu, C. O.; Lichtman, E. I.; Hadler, A. B.; Elrod, M. J. *J. Phys. Chem. A* **2009**, *113*, 221–230.

(28) Yu, J. Z.; Jeffries, H. E.; Sexton, K. G. *Atmos. Environ.* **1997**, *31*, 2261–2280.

(29) Yu, J. Z.; Jeffries, H. E. *Atmos. Environ.* **1997**, *31*, 2281–2287.

(30) Zhao, J.; Zhang, R.; Misawa, K.; Shibuya, K. *J. Photochem. Photobiol. A-Chem.* **2005**, *176*, 199–207.

(31) Birdsall, A. W.; Andreoni, J. F.; Elrod, M. J. *J. Phys. Chem. A* **2010**, *114*, 10655–10663.

(32) Cartas-Rosado, R.; Castro, M. *J. Phys. Chem. A* **2007**, *111*, 13088–13098.

(33) Volkamer, R.; Platt, U.; Wirtz, K. *J. Phys. Chem. A* **2001**, *105*, 7865–7874.

(34) Elrod, M. J. *J. Phys. Chem. A* **2011**, *115*, 8125–8130.

(35) Berndt, T.; Böge, O.; Herrmann, H. *Chem. Phys. Lett.* **1999**, *314*, 435–442.

(36) Olariu, R. I.; Klotz, B.; Barnes, I.; Becker, K.-H.; Mocanu, R. *Atmos. Environ.* **2002**, *36*, 3685–3697.

(37) Grosjean, D. *Sci. Total Environ.* **1991**, *100*, 367–414.

(38) Hofzumahaus, A.; et al. *Science* **2009**, *324*, 1702–1704.

(39) Lou, S.; et al. *Atmos. Chem. Phys.* **2010**, *10*, 11243–11260.

(40) Nehr, S.; Bohn, B.; Fuchs, H.; Hofzumahaus, A.; Wahner, A. *Phys. Chem. Chem. Phys.* **2011**, *13*, 10699–10708.

(41) Tyndall, G.; Cox, R.; Granier, C.; Lesclaux, R.; Moortgat, G.; Pilling, M.; Ravishankara, A.; Wallington, T. *J. Geophys. Res. - Atmos.* **2001**, *106*, 12157–12182.

(42) Aluculesei, A.; Tomas, A.; Schoemaecker, C.; Fittschen, C. *Appl. Phys. B - Lasers Opt.* **2008**, *92*, 379–385.

(43) Kovacs, T.; Blitz, M. A.; Seakins, P. W.; Pilling, M. J. *J. Chem. Phys.* **2009**, *131*, 204304.

(44) Jain, C.; Parker, A. E.; Schoemaecker, C.; Fittschen, C. *ChemPhysChem* **2010**, *11*, 3867–3873.

(45) Fuchs, H.; Bohn, B.; Hofzumahaus, A.; Holland, F.; Lu, K.; Nehr, S.; Rohrer, F.; Wahner, A. *Atmos. Meas. Tech.* **2011**, *4*, 1209–1225.

(46) Craig Markwardt, IDL library, http://cow.physics.wisc.edu/~craigm/idl/, 2010.

(47) Jenkin, M.; Saunders, S.; Wagner, V.; Pilling, M. *Atmos. Chem. Phys.* **2003**, *3*, 181–193.

(48) Bloss, C.; Wagner, V.; Jenkin, M. E.; Volkamer, R.; Bloss, W. J.; Lee, J. D.; Heard, D. E.; Wirtz, K.; Martin-Reviejo, M.; Rea, G.; Wenger, J. C.; Pilling, M. J. *Atmos. Chem. Phys.* **2005**, *5*, 641–664.

(49) Atkinson, R.; Aschmann, S.; Arey, J.; Carter, W. *Int. J. Chem. Kinet.* **1989**, *21*, 801–827.

(50) Klotz, B.; Sorensen, S.; Barnes, I.; Becker, K.-H.; Etzkorn, T.; Volkamer, R.; Platt, U.; Wirtz, K.; Martin-Reviejo, M. *J. Phys. Chem. A* **1998**, *102*, 10289–10299.

(51) Seuwen, R.; Warneck, P. *Int. J. Chem. Kinet.* **1996**, *28*, 315–332.

(52) Moschonas, N.; Danalatos, D.; Glavas, S. *Atmos. Environ.* **1999**, *33*, 111–116.

(53) Klotz, B.; Barnes, I.; Becker, K.-H.; Golding, B. T. *J. Chem. Soc., Faraday Trans.* **1997**, *93*, 1507–1516.

(54) Klotz, B.; Barnes, I.; Becker, K.-H. *Chem. Phys.* **1998**, *231*, 289–301.

(55) Klotz, B.; Barnes, I.; Golding, B. T.; Becker, K.-H. *Phys. Chem. Chem. Phys.* **2000**, *2*, 227–235.

(56) Hoshino, M.; Akimoto, H.; Okuda, M. *Bull. Chem. Soc. Jpn.* **1978**, *51*, 718–724.

(57) Forstner, H.; Flagan, R.; Seinfeld, J. *Environ. Sci. Technol.* **1997**, *31*, 1345–1358.

(58) Huang, M.; Zhang, W.; Hao, L.; Wang, Z.; Zhao, W.; Gu, X.; Guo, X.; Liu, X.; Long, B.; Fang, L. *J. Atmos. Chem.* **2007**, *58*, 237–252.

(59) Huang, M.; Zhang, W.; Hao, L.; Wang, Z.; Fang, L.; Kong, R.; Shan, X.; Liu, F.; Sheng, L. *J. Environ. Sci. - China* **2010**, *22*, 1570–1575.
(60) Gery, M.; Fox, D.; Kamens, R.; Stockburger, L. *Environ. Sci. Technol.* **1987**, *21*, 339–348.
(61) Atkinson, R.; Aschmann, S.; Arey, J. *Int. J. Chem. Kinet.* **1991**, *23*, 77–97.
(62) Bethel, H.; Atkinson, R.; Arey, J. *J. Phys. Chem. A* **2000**, *104*, 8922–8929.
(63) Volkamer, R. A DOAS Study on the Oxidation Mechanism of AromaticHydrocarbons under Simulated Atmospheric Conditions. *Ph. D. thesis*, University of Heidelberg, 2001.
(64) Kwok, E. S. C.; Aschmann, S. M.; Atkinson, R.; Arey, J. *J. Chem. Soc., Faraday Trans.* **1997**, *93*, 2847–2854.
(65) Bandow, H.; Washida, N. *Bull. Chem. Soc. Jpn.* **1985**, *58*, 2541–2548.
(66) Arey, J.; Obermeyer, G.; Aschmann, S. M.; Chattopadhyay, S.; Cusick, R. D.; Atkinson, R. *Environ. Sci. Technol.* **2009**, *43*, 683–689.
(67) Nishino, N.; Arey, J.; Atkinson, R. *J. Phys. Chem. A* **2010**, *114*, 10140–10147.
(68) Wyche, K. P.; Monks, P. S.; Ellis, A. M.; Cordell, R. L.; Parker, A. E.; Whyte, C.; Metzger, A.; Dommen, J.; Duplissy, J.; Prevot, A. S. H.; Baltensperger, U.; Rickard, A. R.; Wulfert, F. *Atmos. Chem. Phys.* **2009**, *9*, 635–665.
(69) Rickard, A. R.; Wyche, K. P.; Metzger, A.; Monks, P. S.; Ellis, A. M.; Dommen, J.; Baltensperger, U.; Jenkin, M. E.; Pilling, M. J. *Atmos. Environ.* **2010**, *44*, 5423–5433.
(70) Bandow, H.; Washida, N. *Bull. Chem. Soc. Jpn.* **1985**, *58*, 2549–2555.
(71) Berndt, T.; Böge, O. *Int. J. Chem. Kinet.* **2001**, *33*, 124–129.
(72) Berndt, T.; Böge, O. *Phys. Chem. Chem. Phys.* **2003**, *5*, 342–350.
(73) Coeur-Tourneur, C.; Henry, F.; Janquin, M.-A.; Brutier, L. *Int. J. Chem. Kinet.* **2006**, *38*, 553–562.
(74) NASA panel for data evaluation. *JPL publication 06-2, evaluation no. 15*; JPL: Pasadena, CA, 2006.
(75) Grosjean, D. *Environ. Sci. Technol.* **1985**, *19*, 968–974.
(76) Atkinson, R.; Aschmann, S.; Arey, J. *Environ. Sci. Technol.* **1992**, *26*, 1397–1403.
(77) Platz, J.; Nielsen, O.; Wallington, T.; Ball, J.; Hurley, M.; Straccia, A.; Schneider, W.; Sehested, J. *J. Phys. Chem. A* **1998**, *102*, 7964–7974.